Bond Performance of Concrete Members Reinforced with FRP Bars

by T. Kanakubo, K. Yonemaru, H. Fukuyama, M. Fujisawa, and Y. Sonobe

Synopsis: An experimental program consisting of three series of tests was conducted in order to investigate the bond performance of concrete members reinforced with FRP bars.

At first, a simple bond test was performed using several types of FRP bars. This test was carried out by pulling out a single bar located near the surface of the concrete block. The test objectives are to evaluate the bond splitting strength of FRP reinforced concrete without lateral reinforcement and to establish a standard test method for bond splitting. Test results show that the bond splitting strength can be estimated using the ratio of lug height to diameter of FRP bars.

In the second test, a bond splitting test was conducted on cantilever type specimens. These were modeled to have the similar stress condition as in a real structure. The test objectives are to study the results of the simple bond test and to evaluate the increment of the bond splitting strength caused by lateral reinforcement. From the test results, the tendency of the bond splitting strength without lateral reinforcement is equal to that obtained from the first test. The increment of the strength caused by lateral reinforcement can be evaluated in terms of its percentage and elastic modulus.

Finally, antisymmetrical loading test for actual beams reinforced with FRP bars was carried out. The obtained bond performance for the longitudinal bars shows a good correlation with the results obtained from the former two tests.

Keywords: Bonding; bond stress; cantilever beams; cracking (fracturing); fiber reinforced plastics; loading tests; reinforced concrete; reinforcing steels; shear strength; tests

Toshiyuki Kanakubo *is a graduate student of doctoral program at the University of Tsukuba, Japan. He received his MEng from the University of Tsukuba in 1991. His main research interests include structural performance of reinforced concrete members using FRP reinforcement.*

Keisuke Yonemaru *is a graduate student of doctoral program at the University of Tsukuba, Japan. He graduated in structural engineering from the University of Tsukuba in 1991. His research interests include bond performance of reinforced concrete members with FRP bars.*

Hiroshi Fukuyama *is a research engineer of Building Research Institute of the Ministry of Construction, Japan. He received his Dr. of Eng from the Science University of Tokyo in 1990. His research interests are in concrete structures, hybrid structures and earthquake–resistant design. He is a secretary of some Comprehensive Technical Development Projects in Japan.*

Masami Fujisawa *is an associate professor in the Department of Architectural Engineering, Tsukuba College of Technology, Japan. He obtained his MEng from Nihon University in 1972. His research areas include structural performance of reinforced concrete members using FRP reinforcement and using high–strength bar.*

ACI member ***Yasuhisa Sonobe*** *is a professor in the Institute of Engineering Mechanics, the University of Tsukuba, Japan. He received his Dr. of Eng from the University of Tokyo in 1959. Currently, much of his research work is on light–weight concrete structures and FRP reinforced concrete members. He is a member of ACI Committee 440; Fiber Reinforced Plastic Reinforcement.*

INTRODUCTION

Bond splitting failure should be avoided to have a good ductility on reinforced concrete members. Especially on FRP reinforced concrete members, a good bond performance is essential to have an effective use of the high tensile strength of bars. While deformed steel bars develop the mechanical bond resistance on lugs, FRP bars develop resistance by several mechanisms. It is considered that the bond resistance can be developed in the same mechanical resistance as steel bars or by frictional resistance between concrete and uneven bar surface. As there are several types of FRP bars, with different shapes, surface treatments and elastic moduli, it is expected that the bond performance of FRP reinforced concrete members would be different from that of steel reinforced concrete members.

The purpose of this research is to investigate the bond performance of FRP reinforced concrete members. Up to now, there are few researches concerning the bond splitting of FRP reinforced concrete members. On the other hand, many data for the bond splitting failure on cantilever type specimens for steel reinforced concrete members have been obtained. To compare with the existing data of steel

bars, a similar cantilever type bond test is selected for the FRP bars. However, this test is fairly difficult to be performed. Also because many types of FRP bars have been developed, a simplified test, that could be a standard bond test, is desirable to study the bond splitting failure. Therefore, a simple bond test [1], by which bond splitting failure can be easily reproduced with a close stress condition to that acting in structural members, is proposed and carried out in parallel with the cantilever type bond test. The test results obtained from the simple bond test are compared with the cantilever type bond test results. Later both test results are confirmed with those obtained from an antisymmetrical loading test for beams.

TEST PROGRAM

Characteristics of FRP Bars

The characteristics of FRP bars used in this research are shown in Table 1. Typical shapes of FRP bars are shown in Fig. 1. Three types of materials of fibers are used in this research; carbon, aramid and glass. Six different shapes are included; straight, braided, deformed, strand, spiral and double spiral type. Sand was applied on the surface of one of the straight and braided type FRP bar. Nominal diameter (D) of FRP bars is provided by each manufacture. A unified definition, the average diameter (d), is used. It is obtained from the measurement of the maximum and minimum diameter at five points along the bar. The lug height (h), that is obtained in a similar way to the case of average diameter, is also used. The values of h, d and h/d are shown in Table 1. The elastic modulus of carbon, aramid and glass FRP bar is about 100~150, 60 and 40GPa, respectively.

Specimens

Dimensions of specimens are shown in Fig. 2. The test variables and this relations to specimen names are shown in Table 2. The size of the simple bond test specimens is 400mm length and 160mm depth. Thickness of the cover concrete is 25mm. The bond length is 15 times of nominal diameter (D). An unbonded region is set at the half part of the specimen. Rubber and a steel plate are placed at the center of the specimen to make the lateral deformation of the bonded concrete not restricted. Normal-weight concrete was cast from the direction as shown in Fig. 2, to set the bar as the bottom side longitudinal bar of a beam. Measured compressive strength of concrete (σ_B) is 44.7 or 49.2MPa.

The size of the cantilever type specimens is 200mm width (b) and 350mm depth, with a bond length of 300mm, that is about 23 times of nominal diameter

(D) of longitudinal bars. Unbonded regions are set at the loaded and free ends of the specimen. Large amount of reinforcement is arranged inside the specimen as shown in Fig. 2, to resist the shear force. The test variables are the types of longitudinal bars and lateral reinforcement, percentage of lateral reinforcement, and concrete type (normal or light-weight concrete). Concrete was cast horizontally from the top side. Measured compressive strength of concrete ranges from 34.5 to 42.7MPa.

The cross section of the beam specimens is 175mm width (b) and 270mm depth. These are designed to be one third scale of the actual beam. The variables are the types of longitudinal bars and lateral reinforcement, percentage of lateral reinforcement, and beam length (shear span ratio M/QD = 2.0 or 2.5). Normal-weight concrete was cast horizontally from the top side. Measured compressive strength is 37.3 or 37.9MPa.

Loading Programs and Measurements

In the cantilever type bond test and the simple bond test as well, longitudinal bars were pulled out monotonically. The loading system used in the cantilever type bond test is shown in Fig. 3 (a). In this test, once the top bars were pulled out, the specimens were turned over and the loading of the bottom bars was carried out in the same way. Pull out load and slip of longitudinal bars at the loaded and free ends were measured in both tests. The loading system used in the antisymmetrical loading test is shown in Fig. 3 (b). Specimens were loaded cyclically by controlling translational angle (R) that is defined as shown in Fig. 3 (b). The loading history to be applied to all specimens is R = ±1/200, ±1/100, ±1/50, ±1/33 radians twice and R = ±1/20, +1/15 radians once. Shear force, relative displacement between the upper and the lower stub and strains of longitudinal bars and lateral reinforcement were measured.

TEST RESULTS

Simple Bond Test

The obtained bond splitting strength (τ_{max}) and failure mode are shown in Table 3. The bond splitting strength is calculated dividing the obtained maximum load by all the bonded area of the bar. Two types of bond resistant mechanisms are considered here as shown in Table 3. One is the bearing resistant type and the other is the friction resistant type. FRP bar with lugs (deformed or spiral shape) belongs to the bearing resistant type. It is considered that the lugs develop the mechanical bond resistance as well as deformed steel bar. Braided or strand shape

bar belongs to the friction resistant type. These bars develop the resistance by friction between concrete and their uneven surface.

Most of the specimens failed by bond splitting, showing cracks along the bar. The obtained bond splitting strength (τ_{max}) of each specimen is shown in Fig. 4. In general, the bond splitting strengths of the bearing resistant type bars are bigger than those obtained for the friction resistant type bars, except the specimen No. 3. Some differences on the bond splitting strength can be observed, even among the same resistant type bars.

Cantilever Type Bond Test

The examples of the bond stress (τ) versus loaded end slip (s) curves are shown in Fig. 5. Combinations of longitudinal bars and lateral reinforcement of the specimens are steel and carbon, both aramid, and both carbon. All specimens failed by bond splitting called side splitting mode as shown in Fig. 5. As the percentages of lateral reinforcement increase, an increment of the maximum bond stress and gradual decrement after the maximum stress can be observed. These phenomena are similar to those observed on the ordinary steel reinforced concrete [2]. Considering the types of longitudinal bars, the maximum bond stresses of FRP bars are smaller than those of steel bars.

Comparison of bond splitting strength obtained between top bars and bottom bars is shown in Fig. 6. The bond splitting strength ratio of top bars to bottom bars is 0.99 among the normal-weight concrete specimens, and 0.91 among the light-weight concrete specimens. The obtained strength for top bars is divided by each ratio to make it comparable to that for bottom bars in later discussions.

Antisymmetrical Loading Test

Shear force (Q) versus translational angle (R) curves with the final crack patterns are shown in Fig. 7. In all specimens, the first crack initiated at the loading cycle of R = 1/200 radians. Shear cracks and bond splitting cracks initiated at the loading cycle of R = 1/100 radians. The maximum loads were observed at R = 1/50 radians, except for specimen S25CC81 that showed the maximum load at R = 1/33 radians. All specimens finally failed by bond splitting. Rupture of FRP bars or yield of steel bars was not observed in the longitudinal bars.

Main results are summarized in Table 4. The observed maximum loads are smaller than the calculated bending strengths because of the bond splitting failure.

BOND SPLITTING STRENGTH OF FRP BARS

Bond Splitting Strength without Lateral Reinforcement

From the results of the simple bond test, some differences on bond splitting strength can be observed even among the bars with the same resistant mechanism as shown in Fig. 4. It can be explained based on the difference of the surface configuration of each FRP bar. Therefore, the bond splitting strength is evaluated using the ratio of lug height to average diameter (h/d). Correlation between the bond splitting strength (τ_{max}) and the value of h/d is shown in Fig. 8. The bond splitting strength is normalized by the square root of the compressive strength of concrete (σ_B unit: MPa). Among the all specimens, as the value of h/d increases, the bond splitting strength also increases in spite of the difference of the resistant mechanisms. The following formula is obtained by regression analysis using the data of the bearing resistant type bars.

$$\tau_{max} / \sqrt{\sigma_B} = 0.67 \, (\, h/d \,)^{0.22} \qquad (1)$$

where, τ_{max} : bond splitting strength (MPa)
σ_B : compressive strength of concrete (MPa)
h/d : ratio of lug height to average diameter of FRP bar (%)

The data for steel bars obtained in a previous study [1, 3] are also shown in Fig. 8. The strengths of bearing resistant type bars are almost the same as steel bars. The strength of friction resistant type bar is 80 ~ 95% of the value calculated by formula (1) except specimen No.3. The bond splitting strength of FRP bars obtained from the simple bond test differs with the bond resistant mechanism type. The strength can be generally evaluated with the value of h/d. It is supposed that the elastic moduli of FRP bars have no influence on the bond splitting strength, because no difference on the strength between carbon, aramid and glass fibers can be appreciated in spite of the different elastic moduli (see Table 3).

In a previous study [2] on bond splitting strength using cantilever type specimens for ordinary steel reinforced concrete members, a formula to predict bond splitting strength was proposed. A further modified formula [4] has been given in case of no lateral reinforcement as follows:

$$\tau_{co} / \sqrt{\sigma_B} = 0.313 \, (\, 0.4 \, b_i + 0.5 \,) \qquad (2)$$

where, τ_{co} : bond splitting strength without lateral reinforcement (MPa)
σ_B : compressive strength of concrete (MPa)
b_i : normalized length of failure line, $= (\, b - N_t \, d_b \,) / N_t \, d_b$
b : width of member
N_t : number of longitudinal bars
d_b : diameter of longitudinal bar

Correlation of the bond splitting strength in the cantilever type bond test between observed values ($_c\tau_{bu}$) and calculated values ($_c\tau_{bu} = \tau_{co}$) using formula (2) is shown in Fig. 9 with the results of regression analysis. The observed values are obtained from specimens without lateral reinforcement for spiral carbon (CFRP13), braided carbon (C128S), braided aramid (K128S), and steel bars. The black marks mean the data of the specimens using normal-weight concrete. As expected, the observed values of steel bars using normal-weight concrete show a good relation with the calculated values. The bond splitting strength of the specimen using light-weight concrete is the same as that obtained for normal-weight concrete in case of no lateral reinforcement. The obtained values of spiral carbon bars have almost the same strength as steel bars, while those obtained for braided carbon and braided aramid bars are about 70% of steel bars. These results show the good accordance with those obtained in the simple bond test, where the bond splitting strength differs with the type of bond resistant mechanism. It is possible to mention that the bond splitting strength can be evaluated using the value of h/d of FRP bars. However, much more data will be necessary to confirm this conclusion.

Increment of Bond Splitting Strength Caused by Lateral Reinforcement

The increment of the bond splitting strength caused by lateral reinforcement (τ_{st}) is defined as follows:

$$\tau_{bu} = \tau_{co} + \tau_{st} \tag{3}$$

where, τ_{bu} : bond splitting strength
τ_{co} : bond splitting strength without lateral reinforcement
τ_{st} : increment of bond splitting strength caused by lateral reinforcement

Where τ_{st} is calculated subtracting τ_{co} from τ_{bu}. In this section, τ_{co} is the calculated values multiplied by the constants shown in Fig. 9 (1, 1, 0.71 and 0.65 in case of steel, spiral carbon, braided carbon and braided aramid bars, respectively). τ_{bu} is separately obtained for each longitudinal bar in the same layer, located at the corner or center of the cross section, using the measured strain. τ_{st} also can be obtained for each longitudinal bar, corner bar or center bar. A formula [4] to predict τ_{st} for ordinary steel reinforced concrete members is given as follows:

$$\tau_{st} = 0.313\,(10\,N_c / N_t + 5\,N_u / N_t) \cdot (b / d_b) \cdot p_w \sqrt{\sigma_B} \tag{4}$$

where, τ_{st} : increment of bond splitting strength (MPa)
N_c : number of corner bars (= 2)
N_u : number of center bars
N_t : number of longitudinal bars
b : width of member

d_b : diameter of longitudinal bar
p_w : lateral reinforcement ratio
σ_B : compressive strength of concrete (MPa)

The constants 10 and 5 are the correlation constants for the corner bars and the center bars, respectively. They are represented as K_c and K_u here after, as they are to be variables due to the types of reinforcements. Discussions about the values of K_c and K_u for FRP reinforced specimens are presented in following sections in both cases for steel longitudinal bars and FRP longitudinal bars as well.

Fig. 10 shows the correlations between τ_{st} and the lateral reinforcement ratio (p_w) for light-weight concrete specimens with steel longitudinal bars and carbon or aramid for lateral reinforcement. The value of ${}_c\tau_{st}$ is normalized by the square root of concrete compressive strength (σ_B). As expected, the values of ${}_c\tau_{st}$ increase with p_w for both types of FRP lateral reinforcements. The increased values for carbon specimens are bigger than those observed for aramid specimens. The correlation values for each specimen are calculated by the least square method and the following formula is obtained.

$$\text{Carbon:} \quad \tau_{st} / \sqrt{\sigma_B} = 0.313\,(6.73\,N_c / N_t + 2.93\,N_u / N_t)\cdot(b / d_b)\cdot p_w \qquad (5)$$

$$\text{Aramid:} \quad \tau_{st} / \sqrt{\sigma_B} = 0.313\,(3.84\,N_c / N_t + 2.12\,N_u / N_t)\cdot(b / d_b)\cdot p_w \qquad (6)$$

The values of K_c are 6.73 and 3.84 in case of carbon and aramid lateral reinforcement, and for K_u are 2.93 and 2.12, respectively. These values are smaller than those for ordinary steel reinforced concrete. It is supposed that the differences of the constants between carbon and aramid, used as lateral reinforcement, are influenced by the elastic modulus. However, the ratios of K_c to K_u are almost the same as that obtained for steel lateral reinforced members (10 : 5 = 2). Therefore, this ratio is fixed at 2, and the ratio of K_c for FRP bars (6.73 or 3.84) to steel (10) is defined as K_{st}. Correlation between the value of K_{st} and the elastic modulus ratio of FRP bars (E_{st}) to steel (E_s) is shown in Fig. 11. The correlation among the data is calculated by the least square method and then formula (7) is proposed. Therefore, formula (8) substitutes formulas (5) and (6).

$$K_{st} = (E_{st} / E_s)^{0.68} \qquad (7)$$

$$\tau_{st} / \sqrt{\sigma_B} = 0.313\,(10\,N_c / N_t + 5\,N_u / N_t)\cdot(b / d_b)\cdot p_w \cdot K_{st} \qquad (8)$$

The same analysis for normal-weight concrete specimens is carried out, and the result is also shown in Fig. 11.

The values of K_c and K_u, that express the increment of bond splitting strength, are shown in Table 5 in case of specimens with FRP longitudinal bars. These constants are calculated similarly as those for specimens with steel longitudinal bars. As shown in Table 5, the values of K_c and K_u differ with the types of longitudinal bars. It is supposed that τ_{st} is influenced not only by the types of lateral reinforcement but also by the types of longitudinal bars. In general, the

values of K_c for FRP longitudinal bars are smaller than those obtained for steel longitudinal bars, then FRP corner bars do not contribute much on the strength, value of τ_{st}.

CORRELATION BETWEEN THE BOND TESTS AND ANTISYMMETRICAL LOADING TEST

Bond capacity is used in following sections as an index that expresses bond splitting strength of members. It is defined as bond splitting strength ($_c\tau_{bu}$) divided by average bond stress ($_c\tau_{ave.}$) for longitudinal bar of member. The value of $_c\tau_{bu}$ is calculated by using the former two bond test results. The value of $_c\tau_{ave.}$ is defined as follows:

$$_c\tau_{ave.} = (\sigma_{ten} - \sigma_{com}) \cdot a_t / (\phi \cdot (L - D)) \quad (9)$$

where, $_c\tau_{ave.}$: average bond stress
σ_{ten} : tensile stress of longitudinal bar at the beam end in the maximum load
σ_{com} : compressive stress of longitudinal bar at the beam end in the maximum load
a_t : area of longitudinal bar
ϕ : perimeter of longitudinal bar
L : clear span length of member
D : depth of member

The maximum load corresponds to the bending strength calculated by fiber analysis [5]. Tensile and compressive stresses of longitudinal bars are also given by fiber analysis. It is supposed that for a member with a bond capacity smaller than 1, it will fail by bond splitting. Bond capacities of 6 beams tested in the antisymmetrical loading test are already shown in Table 4.

Maximum Load of Beams and Bond Splitting Strength

Fig. 12 shows a correlation between bond capacity and the observed maximum load of each beam. The maximum load ($_eQ_{max}$) is normalized by the bending strength ($_cQ_{mu}$) calculated by fiber analysis. The data are located almost on a line, leading to the following formula obtained by the least square method.

$$_eQ_{max} / {}_cQ_{mu} = 0.56\ {}_c\tau_{bu} / {}_c\tau_{ave.} + 0.19 \quad (10)$$

The maximum load of a beam, that fails by bond splitting, can be evaluated using the formula (10) in spite of different types of reinforcement.

Local Bond Performance of Longitudinal Bars

Local bond stress of longitudinal bar is shown in Fig. 13 for the cantilever type bond test. Local bond stress is calculated using the strain obtained from strain gages placed at an interval of 60mm from the loaded end of a longitudinal bar. Specimen L36AA50 is shown as a typical example. The dotted line shows the average bond stress. The location of the section with the maximum stress shifts from the loaded end to the free end as the loading step increases. It is supposed that the reason of a series of splitting failures from the loaded end is due to the small elastic modulus of FRP bars.

Discussions of the local bond performance obtained from beam specimens are as follows. Local bond stress is calculated subtracting of two consecutive strains next to each other. Location of strain gages on longitudinal bar is shown in Fig. 14. T and B mean top bars and bottom bars, respectively. Fig. 15 shows local bond stress (τ) versus the average strain (ε) curves of longitudinal bar in each section of specimen S25CC36. T_{AV} means the average bond stress from the section 1 to the section 4. Dotted lines show the calculated bond splitting strength using the results of the cantilever type bond test. The maximum value of average bond stress (T_{AV}) shows a good relation with the calculated strength. Bigger stresses are observed at some sections, similar as Fig. 13. Local bond stress versus the average strain envelope curves are shown in Fig. 16. The number denotes the position of each section shown in Fig. 14. The dotted curves show the average bond stress from 1 to 3 or 4 according with the specimen. In case of specimens S25SA82 and S25SC81 with steel longitudinal bars, the maximum local bond stresses agree with the calculated values. In case of other specimens with FRP bars, bigger stresses are observed at some sections. It is supposed that these bond performances of longitudinal bars express the characteristics of FRP bars. These performances can be assumed from the results of the cantilever type bond test.

CONCLUSIONS

(1) Two types of bond resistant mechanisms are proposed to study the bond splitting strength of FRP bars. Bond splitting strength of the bearing resistant type bar is almost the same as deformed steel bar. The friction resistant type bar is 80~95% of the bearing resistant type bar in case of the simple bond test. The strength could be evaluated using the ratio of lug height to average diameter of FRP bars.

(2) Elastic modulus of FRP bar has no influence on bond splitting strength in case of the simple bond test.

(3) Bond splitting strength of the cantilever type specimen without lateral reinforcement shows the same tendency of the simple bond test results.

(4) The increment of bond splitting strength caused by lateral reinforcement can be evaluated using elastic modulus of lateral reinforcement in case of steel longitudinal bars. For FRP bars, this increment is influenced not only by the types of lateral reinforcement but also by the types of longitudinal bars.

(5) The maximum load of beams, that fail by bond splitting, can be evaluated by the value of the bond capacity.

(6) Bond performance of beams can be predicted from the results of the cantilever type bond test.

ACKNOWLEDGEMENT

This study was conducted under the National Research Project on the Use of New Materials in Construction Field sponsored by the Ministry of Construction in Japan. The authors gratefully acknowledge the members of the Project for their kind supports.

REFERENCES

[1] Schmidt, G., Stöckl, S., Kupfer, H. : Einfluß einer einachsigen Querpressung und der Verankerungslänge auf das Verbundverhalten von Rippenstählen im Beton, Gefördert mit Forschngsmitteln der Deutschen Forschungsgemeinschaft (DFG) unter dem Kennzeichen Ku 239/39 – 1 und Ku 239/39 – 2, pp. 100 – 174, 1986. 8

[2] S. Morita, H. Fujii : Study on bond splitting strength of deformed bars, Journal of Structural and Construction Engineering, Architectural Institute of Japan, No.408, pp. 45 – 52, 1983. 2 (in Japanese)

[3] J. Furukawa et. al : Bond Test of Deformed Bars embedded in High-strength Concrete, Summaries of technical papers of annual meeting, Structures 2, Architectural Institute of Japan, pp. 371 – 372, 1991. 9 (in Japanese)

[4] Architectural Institute of Japan : Design guidelines for earthquake resistant reinforced concrete buildings based on ultimate strength concept, pp. 135 – 141, 1990 (in Japanese)

[5] K. Mutoh : Plastic design of reinforced concrete structures, Maruzen, Japan, 1967 (in Japanese)

TABLE 1 — CHARACTERISTICS OF FRP BARS

Test Series	Name	Material	Nominal Diameter D(mm)	Shape	Ave. Diameter d(mm)	h/d (%)	Tensile Strength (MPa)	Elastic Modulus (GPa)
Simple bond test	C8ST	Carbon	8φ	Straight	8.01	0.10	1810	147
	C8BR		8φ	Braided	8.75	6.92	1090	98.1
	C10STS		10φ	Straight*1	12.89	7.99	1670	118
	C13DE		13φ	Deformed	13.87	1.95	1460	118
	C10SP		10φ	Spiral	11.03	9.61	1080	108
	C11DE		11–14*2	Deformed	12.94	18.9	628	108
	C12SD		12.5φ	Strand	12.40	6.41	2120	137
	C8DS		8φ	Spiral	10.28	20.5	1770	127
	K128	Aramid	12φ	Braided	11.25	10.9	1290	60.8
	K128S		12φ	Braided*1	12.59	19.9	1290	60.8
	A10SP		10φ	Spiral	10.29	11.1	1320	57.9
	G10SP	Glass	10φ	Spiral	9.89	6.42	883	44.1
	D10	Steel	10φ	Deformed	9.25	8.11	–	–
Cantilever type bond test and Antisym-metrical loading test·	C128S	Carbon	12φ	Braided*1	12.20	7.68	1250	108
	C10'		8φ	Straight	–	–	1140	96.7
	C8'		6φ	Straight	–	–	1130	96.5
	CFRP13		13φ	Spiral	13.30	5.28	1700	130
	CFRP8		8φ	Spiral	–	–	1790	129
	CFRP6		6φ	Spiral	–	–	1620	114
	CFRP4		4φ	Spiral	–	–	1980	149
	K128S	Aramid	12φ	Braided*1	11.50	10.3	1360	58.9
	K64		8φ	Braided	–	–	1330	57.9
	K32		6φ	Braided	–	–	1330	57.9
	G5'	Glass	6φ	Straight	–	–	777	32.2
	D13*3	Steel	13φ	Deformed	13.37	6.81	1120	201
	D13*4		13φ	Deformed	13.37	6.81	963	205

*1 Sand coating *2 Ellipse

*3 Used in the cantilever type bond test (yield stress σ_y=1070MPa)

*4 Used in the antisymmetrical loading test (yield stress σ_y=869MPa)

TABLE 2 — TEST VARIABLES

Test Series	Variables	Fixed Factors
Simple bond test	·Material of longitudinal bar: Carbon, Aramid, Glass, Steel ·Shape of longitudinal bar: Straight, Braided, Deformed, Spiral, Strand	·Bond length: l=15D (D=Nominal diameter) ·Concrete type: Normal-weight ·Concrete compressive strength: σ_B=44.7 or 49.2MPa
Cantilever type bond test	·Longitudinal bar: Carbon-Spiral, Carbon-Braided,Aramid-Braided,Steel ·Lateral reinforcement: Carbon, Aramid, Glass ·Lateral reinforcement ratio: p_w=0 ~ 1.52% ·Concrete type: Light, Normal-weight	·Bond length: l=23, 25D ·Dimension: Width(b) × Depth(D) = 200 × 350mm ·Concrete compressive strength: σ_B=34.5 ~ 42.7MPa
	Name of specimens N36 S C 50 a. b. c. d.	a.Concrete type: N36=Normal, L36=Light b.Longitudinal bar: C=Carbon, A=Aramid, S=Steel c.Lateral reinforcement: C=Carbon, A=Aramid, G=Glass d.Lateral reinforcement ratio: p_w=0.50%
Antisymmetrical loading test	·Longitudinal bar: Carbon-Spiral, Steel ·Lateral reinforcement: Aramid, Carbon ·Lateral reinforcement ratio: p_w=0.36 or 0.81% ·Shear span ratio: M/QD = 2.0 or 2.5	·Dimension: Width(b) × Depth(D) = 175 × 270mm ·Concrete type: Normal-weight ·Concrete compressive strength: σ_B=37.3 or 37.9MPa
	Name of specimens S25 S C 81 a. b. c. d.	a.Shear span ratio: S25=2.5, S20=2.0 b.Longitudinal bar: C=Carbon, S=Steel c.Lateral reinforcement: C=Carbon, A=Aramid d.Lateral reinforcement ratio: p_w=0.81%

TABLE 3 — MAIN RESULTS OF THE SIMPLE BOND TEST

No.	FRP Bar	Bond Resistant Mechanism	Failure Mode	Bond Splitting Strength τ_{max} (MPa)
1	C8ST	Friction	Slip	0.84
2	C8BR	Friction	Bond splitting	5.77
3	C10STS	Friction	Bond splitting	9.30
4	C13DE	Bearing	Bond splitting	4.96
5	C10SP	Bearing	Bond splitting	7.80
6	C11DE	Bearing	Bar rupture	>7.47
7	C12SD	Friction	Bond splitting	5.96
8	C8DS	Bearing	Bond splitting	8.38
9	K128	Friction	Bond splitting	7.55
10	K128S	Friction	Break of coupler	>7.04
11	A10SP	Bearing	Bond splitting	8.46
12	G10SP	Bearing	Bond splitting	7.37
13	D10	Bearing	Bar yield	>7.76

TABLE 4 — MAIN RESULTS OF THE ANTISYMMETRICAL LOADING TEST

No.	Specimen	Calculated Value			Maximum Strength		Failure Mode
		Bending Strength $_cQ_{mu}$ (kN)	Bond Splitting Strength $_c\tau_{bu}$ (MPa)	Bond Capacity $_c\tau_{bu}/_c\tau_{ave.}$	Observed Value $_eQ_{max}$ (kN)	Observed / Calculated $_eQ_{max}/_cQ_{mu}$	
1	S25SA82	156.3	3.98	1.11	112.9	0.79	Bond splitting
2	S25SC81	156.3	4.26	1.19	124.4	0.87	Bond splitting
3	S25CC36	92.8	3.18	0.87	108.7	0.68	Bond splitting
4	S25CC81	92.8	3.69	1.02	119.8	0.75	Bond splitting
5	S20CC36	153.7	3.18	0.66	112.4	0.56	Bond splitting
6	S20CC81	153.7	3.69	0.76	121.7	0.61	Bond splitting

TABLE 5 — VALUE OF K_c AND K_u

Longitudinal Bar	Lateral Reinforcement	K_c	K_u
Carbon–Spiral (CFRP13)	Carbon–Spiral (CFRP6 or 8)	5.69	4.31
Carbon–Braided (C128S)	Carbon–Straight (C8' or C10')	6.63	5.60
Aramid–Braided (K128S)	Aramid–Braided (K32 or K64)	5.96	4.32

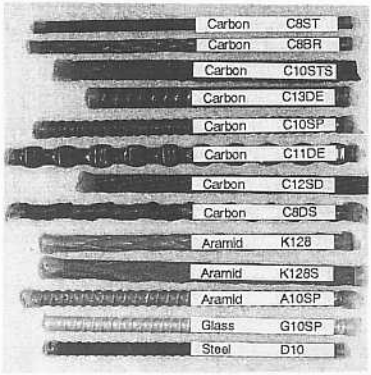

Fig. 1—FRP bars used in the simple bond test

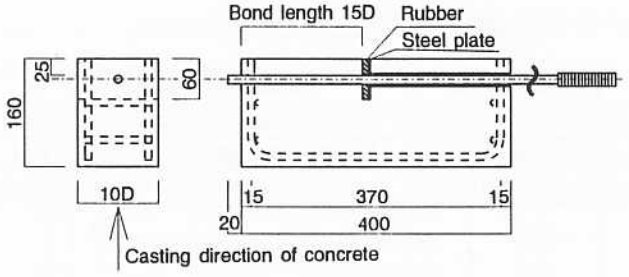

(a) Simple bond test

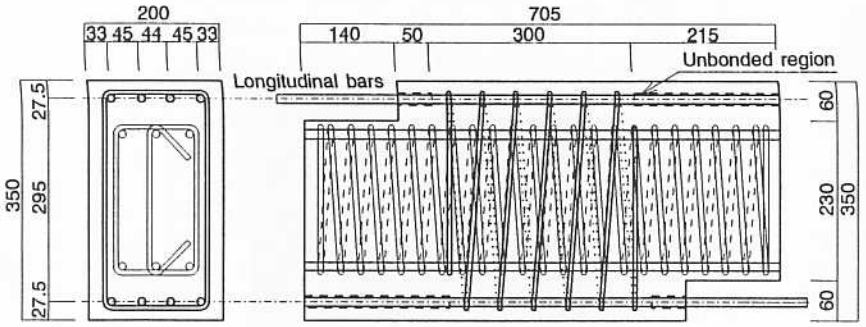

(b) Cantilever type bond test

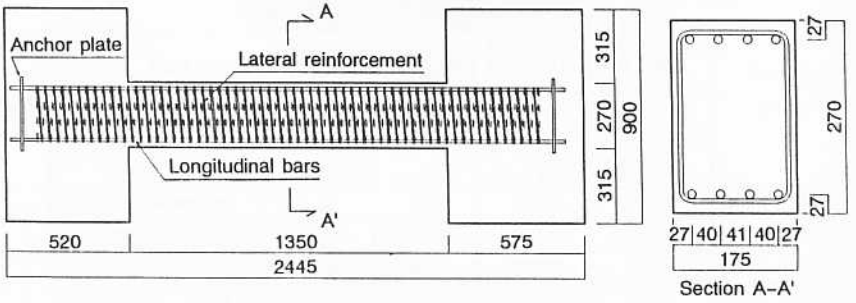

(c) Antisymmetrical loading test

Fig. 2—Dimensions of specimens

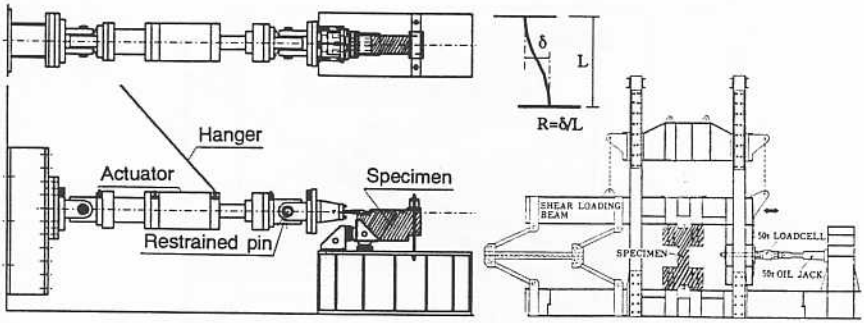

(a) Cantilever type bond test (b) Antisymmetrical loading test

Fig. 3—Loading system

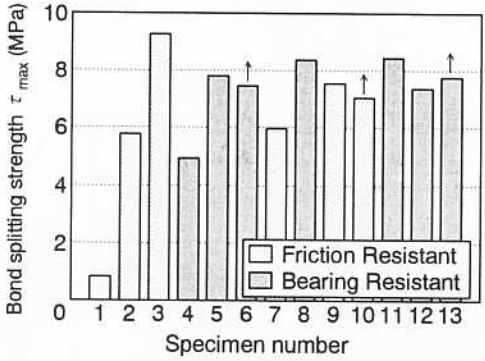

Fig. 4—Bond splitting strength of the simple bond test

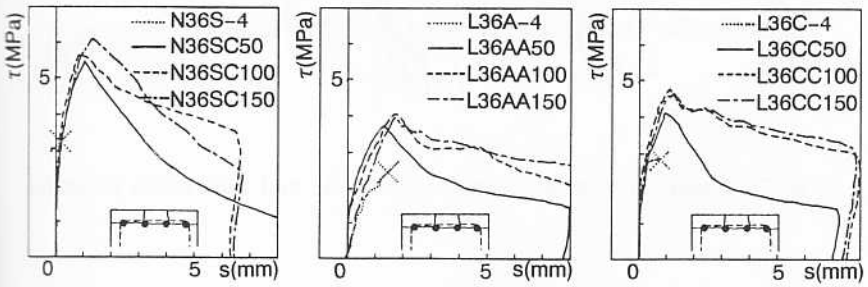

Fig. 5—Bond stress versus loaded end slip curves

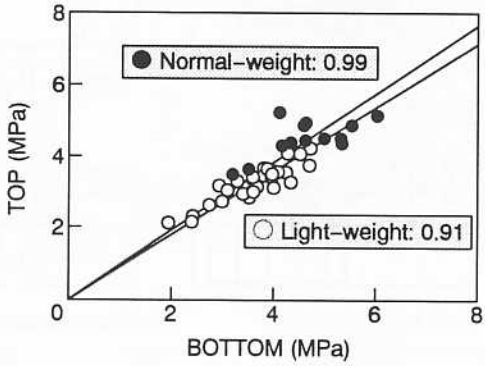

Fig. 6—Comparison of top strength to bottom strength

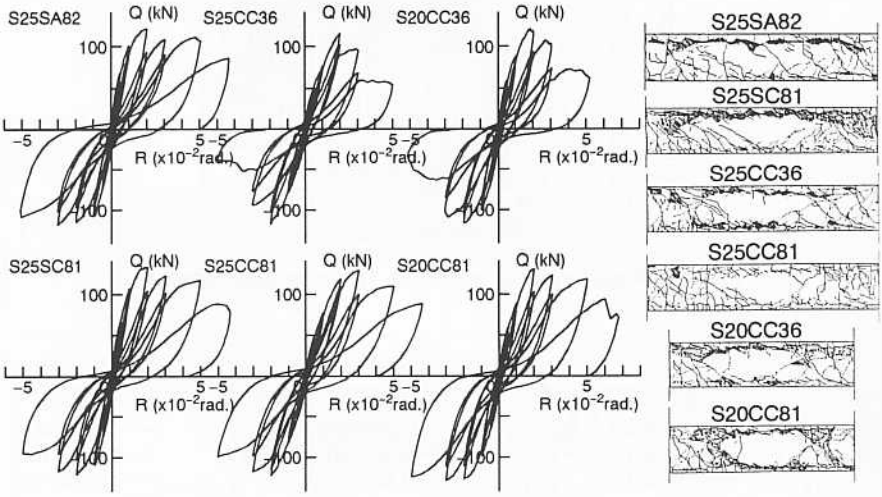

Fig. 7—Shear force-transitional angle curves and final crack patterns

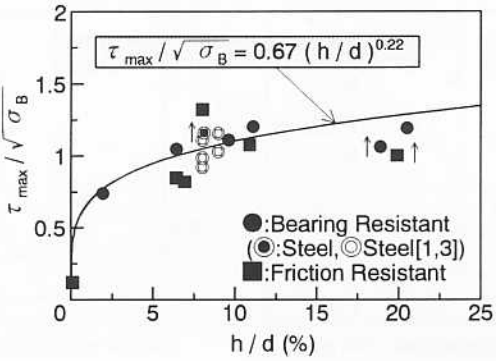

Fig. 8—Bond splitting strength and *h/d*

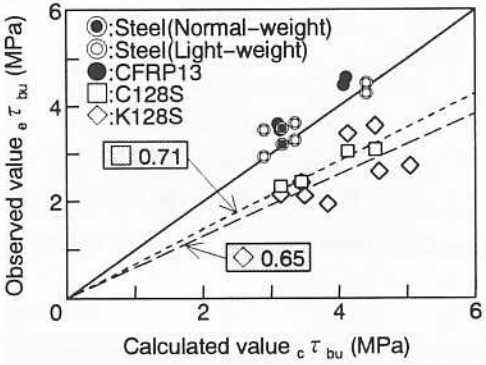

Fig. 9—Comparison of the observed strength to calculated strength

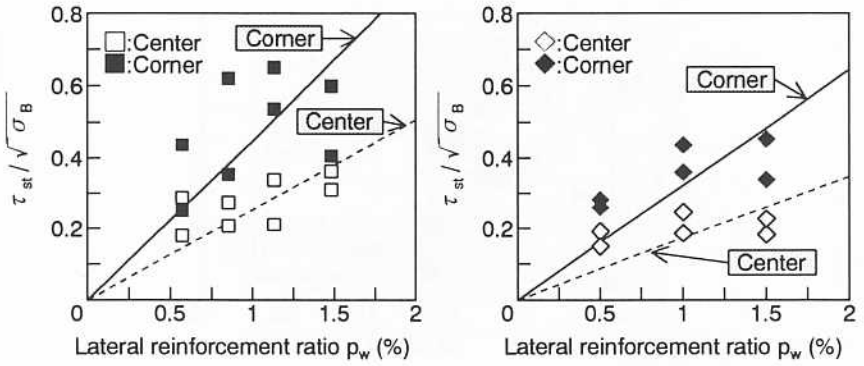

(a) Carbon (b) Aramid

Fig. 10—Correlation between the increment and p_w

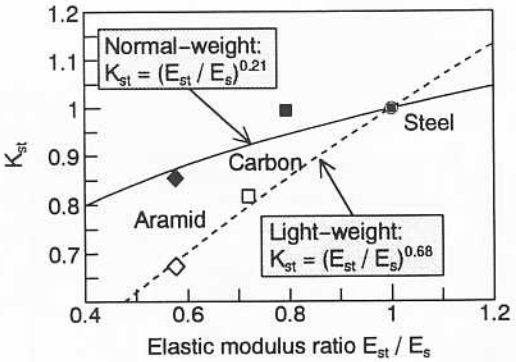

Fig. 11—Correlation between K_{st} and elastic modulus

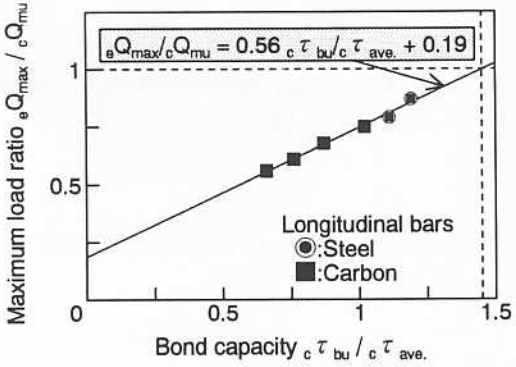

Fig. 12—Correlation between the bond capacity and the maximum load

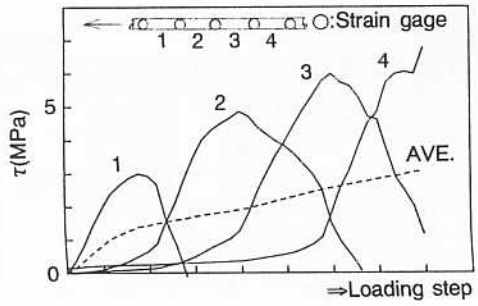

Fig. 13—Transition of local bond stress of cantilever type specimen

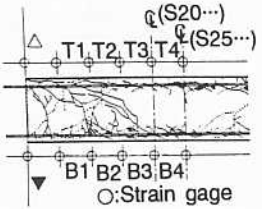

Fig. 14—Location of gages

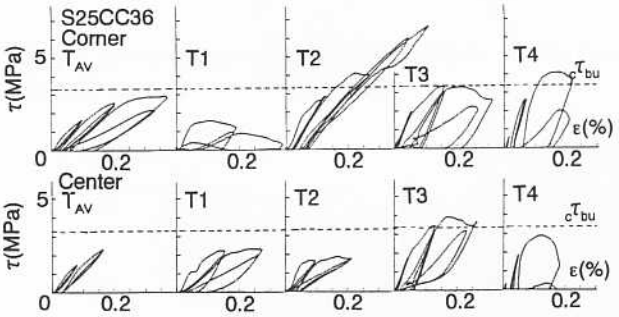

Fig. 15—Local bond stress of beam specimen

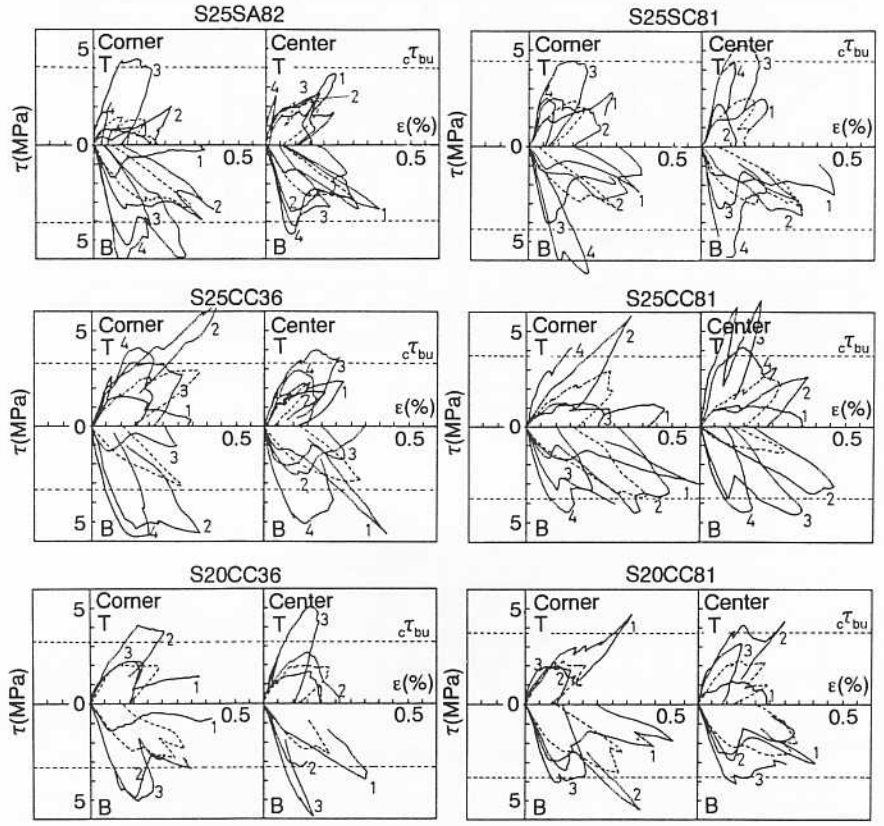

Fig. 16—Local bond stress versus average strain envelope curves